

# Removal of zero-quantum interference in NOESY spectra of proteins by utilizing the natural inhomogeneity of the radiofrequency field

L. Mitschang<sup>a</sup>, J. Keeler<sup>b</sup>, A.L. Davis<sup>b</sup> and H. Oschkinat<sup>a,\*</sup>

<sup>a</sup>European Molecular Biology Laboratory, Meyerhofstrasse 1, 6900 Heidelberg, Germany

<sup>b</sup>Department of Chemistry, University of Cambridge, Lensfield Road, Cambridge CB2 1EW, U.K.

Received 1 July 1992

Accepted 1 September 1992

*Keywords:* Zero-quantum coherence; Inhomogeneity of RF field; Cross relaxation; Interproton distances; Proteins

---

## SUMMARY

A single scan method for the suppression of signals arising from zero-quantum coherences (ZQC) is analysed with respect to its application to NMR experiments on proteins. The ZQC are dephased during a spin-lock period due to the natural RF inhomogeneity of a commercial probe. A quantitative analysis of a ZQC-compensated NOESY experiment is given. Although the build-up curve for the cross peaks in ZQC-compensated NOESY experiments differ from those in uncompensated experiments, interproton distances in medium-sized proteins can be evaluated with high accuracy. The proposed method is compared with other techniques for ZQC suppression.

---

## INTRODUCTION

Structure determination of proteins by Nuclear Magnetic Resonance relies on the quantitative interpretation of NOESY spectra to obtain a set of distances from which structures can be calculated. There are various approaches for converting the information contained in the cross-peak amplitudes into distances, ranging from approximation approaches ('initial rate approximation') to treatments by means of a relaxation matrix. In all cases, it is necessary to record NOESY spectra with short mixing times, whereby so-called J cross peaks (Macura et al., 1981) become visible, as they are not sufficiently attenuated by relaxation during the short mixing period. J cross peaks, which originate from zero-quantum coherences (ZQC), cannot be compensated for by proper phase cycling or the application of pulsed field gradients (Wokaun and Ernst, 1977; Bax et al., 1980; Bodenhausen et al., 1984). They are usually very broad because of their dispersive line

---

\* To whom correspondence should be addressed.

shapes and may therefore cause severe problems in NOESY spectra of proteins, especially when adjacent cross peaks are to be integrated or when NOE between coupled protons are of interest. In general, signals with phase distortions due to ZQC occur whenever in-phase magnetization and z-magnetization ( $(I_x) \xrightarrow{90^\circ_y} (I_z)$ ) are interchanged, as the accompanying anti-phase magnetization is then interchanged with ZQC ( $(2I_{1y}I_{2z} - 2I_{1z}I_{2y}) \xrightarrow{90^\circ_y} (2I_{1y}I_{2x} - 2I_{1x}I_{2y})$ ), e.g., z-filtered experiments (Sørensen et al., 1984). However, the fact that the ZQC precess during mixing time may be used to reduce their contribution to a tolerable level by adding several experiments with various effective precession periods (Macura et al., 1981; Sørensen et al., 1984; Rance et al., 1985; Otting 1990).

In this paper, we discuss a recently proposed alternative method for zero-quantum suppression (Titman et al., 1990) as applied to proteins. We place special emphasis on the NOESY experiment, including its quantitative analysis. The method allows the effective suppression of ZQC in one scan and throughout the whole spectrum except in a region around the diagonal.

In this method, the ZQC are dephased by a  $B_1$ -gradient during a 'spin-lock' period. When a cw RF field is applied, the component of the magnetization which points along the direction of the effective field is said to be 'spin locked'. This means that this component is affected by relaxation, but does not precess. In contrast, the orthogonal components do precess with a frequency proportional to  $p(\gamma B_1)$  for  $p \neq 0$ , where  $p$  is the order of coherence (Bodenhausen, 1981). In this case, the spatial inhomogeneity of the RF field causes a distribution of precession frequencies across the sample and leads to 'fanning out' of the precessing components, where coherences of one order or higher decay rapidly. By comparison, ZQC are much less affected by RF inhomogeneity because their precession frequency is proportional to the difference between the effective fields of the two coupled spins. However, the dephasing of ZQC can be optimized by choosing a resonance offset for the spin lock for which their precession frequencies have maximum sensitivity to RF inhomogeneity.

The dephasing of ZQC by a cw RF field for two coupled nuclei of the same species is analysed in the next section. It turns out that there is a well-defined resonance offset  $\zeta_{\text{opt}}$  for the spin lock to be most effective in the dephasing of ZQC. The rate of dephasing is proportional to the difference in Larmor frequency of the two coupled spins and to the RF inhomogeneity across the sample. To achieve optimal dephasing of ZQC in a short time, Titman et al. (1990) used a probe with a special coil to produce a strongly inhomogeneous  $B_1$  field. As this causes some experimental difficulties, it is preferable to do the experiment with an unmodified probe, especially when water suppression becomes important. It will be shown here that the dispersion of Larmor frequencies in protein spectra and the natural inhomogeneity of the RF field of a commercial probe enables the dephasing of ZQC in a reasonable time at high Zeeman fields (600 MHz); no modification of the probe is necessary.

The spin lock can be included into any z-filter-like scheme (Sørensen et al., 1984) to establish the exclusive transfer of in-phase magnetization to z-magnetization, or vice versa, in a single scan (Titman et al., 1990). For this purpose, the in-phase magnetization is rotated about an appropriate angle by a hard pulse to be aligned parallel to the effective field, where it is spin locked at the optimal resonance offset  $\zeta_{\text{opt}}$ . After sufficient time has elapsed for dephasing of all components, including ZQC, the  $90^\circ$  rotation is completed by another hard pulse. In this way, in-phase magnetization is transformed to z-magnetization and any other coherence transfer usually induced by a  $90^\circ$  hard pulse is suppressed (Fig. 1A). Alternatively, an adiabatic pulse can be used (Ugurbil et

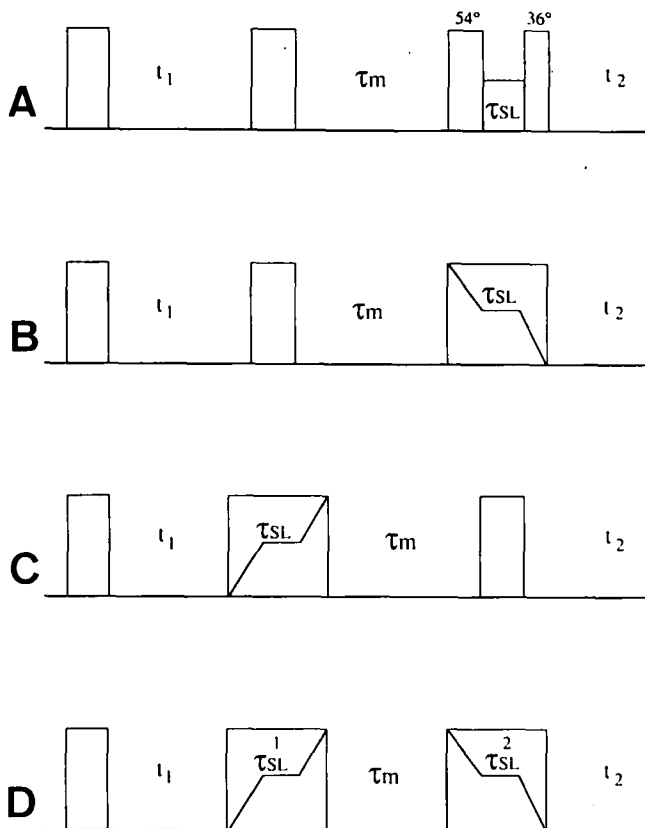


Fig. 1. Different experimental set-ups for the ZQC-compensated NOESY experiment. In (A), the read pulse of the NOESY sequence is substituted by a  $54.7^\circ$  hard pulse, the spin lock, and a  $35.3^\circ$  hard pulse to accomplish the  $90^\circ$  rotation from the z-axis to the xy-plane. Sequence (B) utilizes an adiabatic pulse for this purpose. The frequency sweep starts from 500 kHz off resonance, approaches the point where the tilt angle of the magnetization is  $54.7^\circ$ , stays there during a spin-lock period of several milliseconds, and afterwards completes the  $90^\circ$  rotation of the magnetization by sweeping on resonance. The actual sweep (without spin lock) was performed in  $330 \mu\text{s}$ , with the frequency being changed in a tangential manner. In (C) dephasing is achieved during the second pulse of the NOESY sequence, but now the sweep starts on resonance and ends off resonance. Sequence (D) employs two adiabatic pulses with spin locking at the magic angle. For  $\tau_{\text{SL}}^1 + \tau_{\text{SL}}^2 = \tau_{\text{SL}}$ , this sequence is in principle equivalent to the previous ones, but cannot be recommended due to the additional mixing process (see text).

al., 1988; Titman et al., 1990). To achieve an  $x \rightarrow z$  rotation for example, in-phase magnetization is initially spin locked on resonance along the x-axis. The frequency of the RF field is then moved off resonance, causing the spin-lock axis (the effective field) to move towards the z-axis. If the adiabatic condition (Abragam, 1961) is met, the in-phase magnetization remains spin locked and is transformed to z-magnetization at the end of the frequency sweep, when a large resonance offset is applied. The dephasing of ZQC and other coherences, which are not spin locked, can easily be managed by halting the frequency sweep at the desired offset  $\zeta_{\text{opt}}$  for sufficient time.

ZQC arise in NOESY experiments only from antiphase magnetization evolving during  $t_1$ . They can be suppressed by including one of the two schemes mentioned above before detection. Three pulse sequences for such a ZQC-compensated NOESY experiment are shown in Figs. 1A, B and

C. In principle, ZQC could also be compensated for by using the pulse sequence 1D. However, this sequence has disadvantages, especially when molecules with large NOEs are investigated, as discussed below.

All these techniques should be applied to proteins with caution, as the ROE arising in the spin-lock period interferes with the NOE whose build-up curve should preferably be measured (Kumar et al., 1981). This curve, however, is a little different in a compensated experiment than in a normal NOESY, and depends on the molecule investigated. For proteins, negative cross peaks are observed at zero NOE mixing time and, for increasing NOE mixing time, the intensities pass through zero in the linear part of the build-up curve. The slope of the linear part of the curve is affected when the spin-lock duration is too long. As an example, build-up curves were recorded for the basic pancreatic trypsin inhibitor (BPTI). However, it is shown that the experimental parameters can be chosen accurately enough to yield correct results.

## THEORY

The spin locking of in-phase magnetization and the precession of ZQC around the effective field is best described in a tilted frame of reference, whose z-axis lies in the direction of the effective field. The in-phase magnetization in the rotating frame becomes longitudinal magnetization in the tilted frame and the antiphase magnetization transforms to ZQC. For two coupled nuclei, *i* and *j*, of the same species, the latter precesses around the z-axis of the tilted frame with a frequency given by the difference of the effective fields (Bazzo and Boyd, 1987; Titman et al., 1990)

$$\begin{aligned}\Omega_{ZQ} &= \{\Omega_i^2 + \omega_1(r)^2\}^{1/2} - \{\Omega_j^2 + \omega_1(r)^2\}^{1/2} \\ &= \{(\zeta + \delta)^2 + \omega_1(r)^2\}^{1/2} - \{(\zeta - \delta)^2 + \omega_1(r)^2\}^{1/2}\end{aligned}\quad (1)$$

where  $\Omega_i$  and  $\Omega_j$  are the resonance offsets of the nuclei *i* and *j*, respectively,  $\omega_1$  is the spin-lock power,  $\zeta = (\omega_{i0} + \omega_{j0})/2 - \omega$  and  $\delta = (\omega_{i0} - \omega_{j0})/2$ , where  $\omega$  is the transmitter frequency,  $\omega_{i0}$  and  $\omega_{j0}$  are the Larmor frequencies of the nuclei (i.e.,  $\Omega_i = \zeta + \delta$  and  $\Omega_j = \zeta - \delta$ ). In Eq. 1 an effective coupling constant is neglected (Bazzo and Boyd, 1987), because it is very small compared to the operative frequencies  $\Omega_i$ ,  $\Omega_j$  and  $\omega_1$ . For a spin lock on resonance ( $\zeta = 0$ ),  $\Omega_{ZQ}$  is zero and also in the limit of very large offsets ( $\zeta \gg \omega_1$ ). For an intermediate offset,  $\Omega_{ZQ}$  depends on  $\omega_1(r)$  and therefore on the spatial field distribution  $B_1(r)$ , indicated by the position coordinate *r*. This causes a spread of ZQ precession frequencies across the sample. For a sufficiently long spin lock, the resultant ZQ contribution decays by dephasing. The intermediate offset  $\zeta$  for the quickest dephasing rate is calculated as the offset  $\zeta_{opt}$ , where the derivative of  $\Omega_{ZQ}$  with respect to  $\omega_1$  is maximum as a function of offset  $\zeta$ . The solution is

$$\zeta_{opt} = \omega_1/2^{1/2}\quad (2)$$

Second-order and higher ( $\delta/\omega_1$ ) terms are neglected, which gives a good approximation as long as  $|\omega_{i0} - \omega_{j0}| \leq (\omega_1/4)$ . Each nucleus is locked along the direction of its effective field, described by the tilt angles

$$\Theta_i = \arctan\{\omega_1/\zeta + \delta\}$$

$$\Theta_j = \arctan\{\omega_1/\zeta - \delta\} \quad (3)$$

between the z-axis of the rotating frame and the z-axis of the tilted frame. The optimal direction of the spin lock is therefore

$$\Theta_{\text{opt}} \approx \arctan\{\omega_1/\zeta_{\text{opt}}\} = 54.7^\circ \quad (4)$$

with  $\Theta_i \approx \Theta_j \approx \Theta_{\text{opt}}$  for  $\zeta > \delta$ . Setting the offset close to the magic angle is therefore not critical.

The range of ZQ oscillation frequencies over the sample,  $\Delta\Omega_{\text{ZQ}}$ , is given by

$$\Delta\Omega_{\text{ZQ}} = \{\Delta\Omega_{\text{ZQ}}(\zeta_{\text{opt}}/z)/d\omega_1\}\Delta\omega_1. \quad (5)$$

$\Delta\omega_1$  is the range of values for  $\omega_1$  (or  $B_1$ ) apparent in the sample (a more detailed analysis requires volume integration).

We have measured the  $\omega_1(r)$ -characteristic of our spectrometer (Bruker AMX 600) in a two-dimensional experiment (Bax, 1982). Our standard 5-mm proton probe is equipped with a Helmholtz coil for excitation and detection. The  $\omega_1$ -distribution is a folding of the actual  $B_1$  inhomogeneity and the detection characteristic of the coil, as sites excited with weak  $B_1$  are also detected but with poor efficiency. As this distribution is not symmetrical, the indicated range,  $\Delta\omega_1$ , is estimated as the width of the  $\omega_1$ -distribution around the nominal  $\omega_1$  ( $B_1$ ) strength, which includes 80% of the integral of the  $\omega_1$ -distribution. The nominal  $\omega_1$  strength, called  $\omega_{1*}$ , is measured with a  $90^\circ$  hard pulse. In this way, the ratio  $(\Delta\omega_1/\omega_{1*}) \approx 0.4$  and is approximately independent of the adjusted transmitter power ( $\omega_{1*}$  values from 2 to 15 kHz have been tested).

Under the conditions of Eq. 2, again neglecting higher orders in  $(\delta/\omega_1)$ ,

$$d\Omega_{\text{ZQ}}(\zeta_{\text{opt}}, \omega_{1*})/d\omega_1 = (4/3^{3/2})(\delta/\omega_{1*}) \quad (6)$$

and the range of ZQC oscillation frequencies for  $\Delta\omega_1 \approx 0.4 \omega_{1*}$  becomes

$$\Delta\Omega_{\text{ZQ}} \approx (\omega_{i0} - \omega_{j0})/6 \quad (7)$$

The dephasing rate depends on the difference in Larmor frequencies of the two coupled nuclei and therefore on the strength of the applied Zeeman field. (Equation 7 is valid for the experimental conditions used in our study (natural RF inhomogeneity). The denominator would decrease ( $\Delta\Omega_{\text{ZQ}}$  increase) for a stronger RF inhomogeneity, Eq. 5, which could be provided, for example, by a modified probe.)

As ZQC precess at different rates with different frequencies according to Eq. 7, they cancel each other after a spin-lock duration  $\tau_{\text{SL}}$  determined by

$$\Delta\Omega_{\text{ZQ}} \tau_{\text{SL}} \approx 2\pi \quad (8)$$

$\tau_{\text{SL}}$  is the shortest duration of a spin lock at the resonance offset  $\zeta_{\text{opt}}$  which can dephase ZQC and all higher order coherences for a given pair of coupled spins.

For a ZQC-compensated NOESY experiment, the spin lock can be inserted into the pulse sequence in various ways, as shown in Fig. 1. In the following, the cross-peak intensity is analysed for the sequences of Figs. 1A and 1B as a function of  $\tau_{\text{SL}}$  and  $\tau_m$  (the results for the experiment reported in Fig. 1C can be obtained by interchanging the indices in the following calculation). We assumed only dipole-dipole interactions between pairs of spins, isotropic motion, and, as the spin lock is applied off resonance, energy mismatch conditions (no TOCSY transfer). During  $\tau_m$ , the exchange of z-magnetization,  $(I_{iz})$ , is governed by the relaxation rates,  $\Gamma$ , for magnetization, which is longitudinal in the rotating frame. At the end of  $\tau_m$ ,  $(I_{iz})$  is moved by an adiabatic sweep or a hard pulse to the direction of the effective field where it is locked (Eq. 3) and transforms to  $(I_{ix}\sin\Theta_i + I_{iz}\sin\Theta_i)$ . During  $\tau_{\text{SL}}$ , only terms that commute with the spin-lock Hamiltonian, like the former, cross relax. Other commuting terms were not investigated as they cause well-known offset effects in rotating-frame cross-relaxation experiments and can be compensated for (Griesinger and Ernst, 1987). The terms which do not commute with the spin-lock Hamiltonian decay are due to RF inhomogeneity. Magnetization transfer between locked components which are longitudinal in the tilted frame is governed by the relaxation rates  $\Gamma^i$  (Griesinger and Ernst, 1987).

The intensity of the cross-peak between spin  $i$  and  $j$  is given by

$$a_{ij}(\tau_m + \tau_{\text{SL}}) = \sum_n [\exp\{-\Gamma^i \tau_{\text{SL}}\}]_{in} [\exp\{-\Gamma \tau_m\}]_{nj} M_{j0} \quad (9)$$

where  $M_{j0}$  is the thermal equilibrium magnetization of spin  $j$  and the summation runs over all spins. An initial rate approximation for both mixing periods gives the cross-peak integral

$$a_{ij}(\tau_m + \tau_{\text{SL}}) = \{-\Gamma^i_{ij} \tau_{\text{SL}} - \Gamma_{ij} \tau_m + [\Gamma^i_{ij} \Gamma_{ij} + \Gamma^i_{ij} \Gamma_{jj} + \sum_k \Gamma^i_{ik} \Gamma_{kj}] \tau_m \tau_{\text{SL}}\} M_{j0} \quad (10)$$

The first and the second terms represent magnetization which arises from cross relaxation between the spins  $j$  and  $i$  during  $\tau_{\text{SL}}$  and  $\tau_m$ , respectively. The first term in the inner bracket represents magnetization which arises from cross relaxation during  $\tau_m$  and relaxation during  $\tau_{\text{SL}}$ . The second term in the inner bracket represents magnetization which relaxes during  $\tau_m$  and further cross relaxes during  $\tau_{\text{SL}}$ . The final term in the inner bracket represents magnetization which starts from spin  $j$  and cross relaxes with spin  $k$  during  $\tau_m$ . The magnetization on spin  $k$  is then transferred to spin  $i$  by further cross relaxation during  $\tau_{\text{SL}}$ . It represents the indirect relaxation pathways between spin  $j$  and  $i$  via any other spin  $k$ . The summation runs over all  $k$  other than  $j$  and  $i$ .

In order to obtain distances from ZQC-compensated NOESY, the intensities of the cross peaks are measured at different mixing times,  $\tau_m$ . The duration of the spin lock,  $\tau_{\text{SL}}$ , is kept constant to ensure the suppression of ZQC. Such a build-up curve has a linear slope proportional to

$$-\Gamma_{ij} + [\Gamma^i_{ij} \Gamma_{ij} + \Gamma^i_{ij} \Gamma_{jj} + \sum_k \Gamma^i_{ik} \Gamma_{kj}] \tau_{\text{SL}}. \quad (11)$$

The distance between spins  $i$  and  $j$  can be evaluated from the linear slope if the first term in Eq. 11 dominates, as  $\Gamma_{ij}$  is the only term solely depending on this distance. The terms in the bracket depend on the distances from spins  $j$  and  $i$  to all other spins, because of external relaxation, described by the relaxation rates with like indices, or because of direct cross relaxation with other spins,  $k$ . However, the significance of these terms is controlled by the length of the spin-lock

period,  $\tau_{\text{SL}}$ . It is therefore desirable to choose a  $\tau_{\text{SL}}$  as short as possible, while maintaining the condition  $\Delta\Omega_{\text{ZQ}} \tau_{\text{SL}} \approx 2\pi$ , Eq. 8.

In general, when using the proposed technique for ZQC-suppression, it is necessary to compensate for the ROE resulting from the spin lock. For molecules with negative NOE ( $\omega_0 \tau_c > 1.12$ ), the cross-relaxation rate,  $\Gamma_{ij}$ , may have the opposite sign to the cross-relaxation rate,  $\Gamma_{ij}^{\text{u}}$ , depending on the tilt angle of the effective fields (Eq. 3). The solution  $\zeta_{\text{opt}}$  in Eq. 2 is valid for a moderate spin-lock power ( $\omega_1 \geq 4|\omega_{i0} - \omega_{j0}|$ ) and yields roughly  $\Theta_i \approx \Theta_j \approx \Theta_{\text{opt}}$  because  $\zeta > \delta$ . In the slow motion limit ( $\omega_0 \tau_c \gg 1$ ), which is valid for proteins,  $\Gamma_{ij}^{\text{u}} = -\Gamma_{ij}$  for an offset  $\zeta_{\text{opt}}$ , and the build-up of cross-peak intensity during the spin lock can be compensated for by setting  $\tau_m = \tau_{\text{SL}}$ . However, satisfactory results are only obtained when the relaxation behaviour of the spins is very similar.

## EXPERIMENTAL

The sample consisted of a 7 mM solution of BPTI in 90% H<sub>2</sub>O/10% D<sub>2</sub>O, pH 3.6. The temperature was 303 K.

ZQC-compensated NOESY experiments were recorded with the pulse sequence shown in Fig. 1B. Water suppression was achieved by presaturation. The spectrometer (Bruker AMX 600) was equipped with a standard triple-resonance probe. The length of the 90° pulses was 8.2  $\mu\text{s}$ . The adiabatic pulse consisted of a cascade of pulses with different frequencies, but a preserved phase. Alternatively, the phase may be changed to obtain the desired sweep. The adiabatic pulse was given with a nominal field strength of 8.3 kHz, starting at 500 kHz off resonance (relative to the water frequency) and approaching the resonance offset of 5799 Hz relative to the water signal in 20 steps with tangential changes in frequency (Hardy et al., 1986). The spin lock for dephasing the ZQC ( $\tau_{\text{SL}}$ ) was applied at that offset. The 90° rotation of the locked magnetization was completed with another 12 steps until the resonance frequency of water was reached, the frequency again changing in a tangential manner. Three series with different spin-lock durations and variable short mixing times were recorded:  $\tau_{\text{SL}} = 5$  ms and  $\tau_m = 0$  ms, 5 ms, 10 ms, 25 ms, 45 ms;  $\tau_{\text{SL}} = 10$  ms and  $\tau_m = 0$  ms, 10 ms, 30 ms, 50 ms;  $\tau_{\text{SL}} = 20$  ms and  $\tau_m = 0$  ms, 20 ms, 30 ms, 40 ms, 60 ms. One series of normal NOESY experiments without ZQC suppression and with  $\tau_m = 10$  ms, 20 ms, 40 ms, 60 ms was also performed. In all experiments, 2048 data points were collected in  $t_2$ ; the spectral width was 8333 Hz. 512  $t_1$  increments with 32 scans each were taken with a 32-step phase cycle to compensate for axial peaks, double-quantum signals and quadrature images in the uncompensated NOESY experiments, but 8 scans per  $t_1$  increment and a 8-step phase cycle to compensate for axial peaks and double-quantum signals (DQC) only were used for the ZQC-compensated experiments. The phase cycle for the removal of DQC in the compensated experiment is in principle not necessary, but was chosen to make sure that an undisturbed view of the residual signals due to ZQC was given.

The B<sub>1</sub>-inhomogeneity was determined on a selective proton probe with a 600 MHz spectrometer (Bax, 1982), using B<sub>1</sub> fields of different strength. We assume that the inhomogeneity is comparable to that of the triple-resonance probe used to record the spectra.

## RESULTS AND DISCUSSION

The efficiency of zero-quantum suppression by off-resonance spin locking was tested with

BPTI. The fingerprint regions of two compensated NOESY experiments ( $\tau_{\text{SL}} = 10$  ms) are shown in Fig. 2, one with a NOESY mixing time of  $\tau_{\text{m}} = 10$  ms, and the other with a NOESY mixing time of  $\tau_{\text{m}} = 30$  ms (Figs. 2A and 2B). Uncompensated NOESY experiments with mixing times of 0 and 20 ms are also shown for comparison. The spectra were recorded in a sequential manner and show normalized peak amplitudes. The compensated spectrum recorded with a NOE mixing

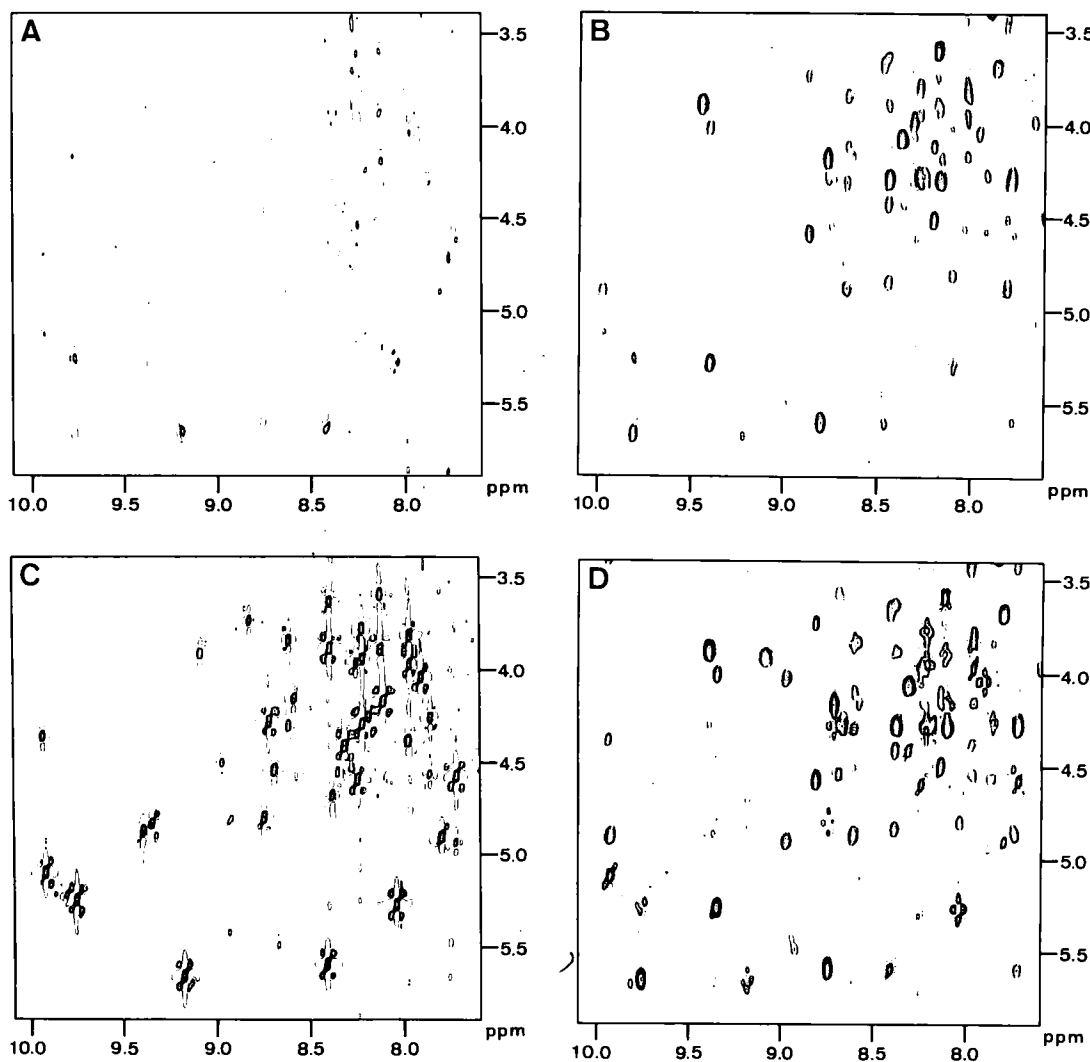


Fig. 2. Fingerprint regions of ZQC-compensated NOESY spectra of BPTI (Aprotinin) (A and B) recorded with the pulse sequence in Fig. 1B employing a spin lock of  $\tau_{\text{SL}} = 10$  ms and NOESY mixing times of  $\tau_{\text{m}} = 10$  ms and  $\tau_{\text{m}} = 30$  ms, respectively. For comparison, normal NOESY experiments with mixing times of 0 ms and 20 ms are shown in (C) and (D). Negative signals are shown with only one contour, whereas positive signals are contoured in a logarithmic manner. The spectra were normalized to enable a direct comparison of the peak amplitudes. Spectrum (A) demonstrates the effective suppression of ZQC by a spin lock of 10 ms but shows significant ROE signals. The efficiency of the suppression can be seen by comparing the NOESY spectra shown in (C) and (D). The latter spectrum shows relatively strong signals due to ZQC even at a mixing time of 20 ms. Spectrum (B) is comparable to the normal NOESY spectrum shown in (D).



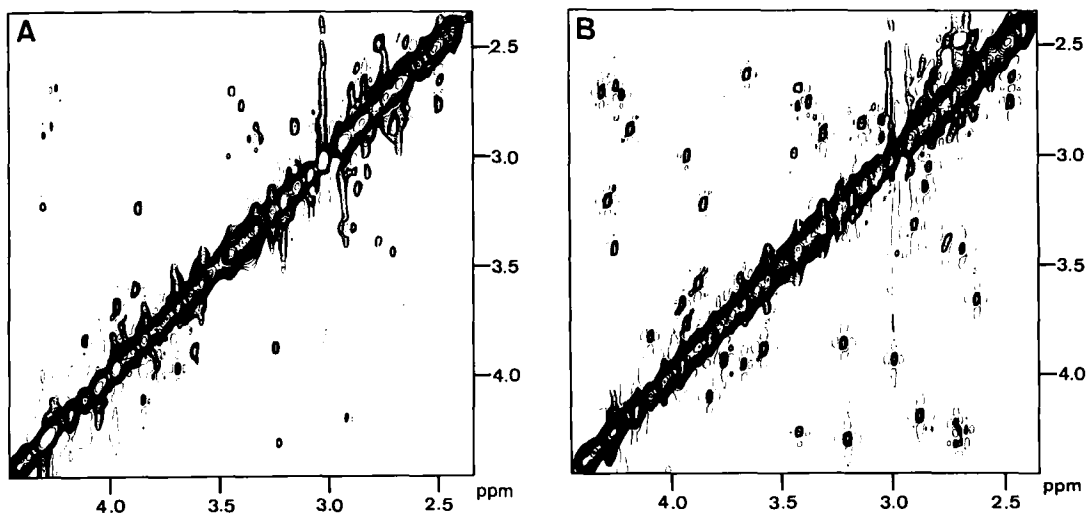


Figure 3. (A) Part of the aliphatic region of the ZQC-compensated spectrum shown in Fig. 2A and of the normal NOESY spectrum with zero mixing time (B). The efficiency of suppression decreases the closer the cross peaks appear to the diagonal. With the spin-lock time used ( $\tau_{\text{SL}} = 10$  ms), cross peaks due to ZQC of coupled spins with a difference in precession frequencies smaller than 600 Hz are only partially suppressed.

time of  $\tau_m = 10$  ms (Fig. 2A) shows very little ROE and may be compared with the NOESY spectrum with zero mixing time shown in Fig. 2C, which shows the J-peaks in full size, and with the NOESY spectrum in Fig. 2D, which shows a normal NOESY spectrum recorded with 20 ms mixing time and still relatively strong signals due to ZQC. The point where zero ROE/NOE is observed in the compensated spectra was determined to be  $\tau_m = 14$  ms for  $\tau_{\text{SL}} = 10$  ms, instead of  $\tau = 10$  ms (see above). This is partly dependent on the offset of the locked resonances from the carrier ( $\Theta_i, \Theta_j \neq \Theta_{\text{opt}}$ ) and the local correlation times, hence a sharp null is not observed. The compensated experiment recorded with a mixing time of  $\tau_m = 30$  ms already shows substantial NOEs and is, to some extent, comparable to the spectrum in Fig. 2D. It shows, however, slightly smaller amplitudes for most signals, which is partly because it took 14 ms for ROE compensation and therefore the 'effective NOE mixing time' was only 16 ms. The smaller amplitudes are also because of the loss of magnetization during  $\tau_{\text{SL}}$  and  $\tau_m$ . There is, however, also a large difference between these two spectra, namely the absence of NOE involving the NH of Arg<sup>39</sup> and Thr<sup>11</sup> at 9.08 and 8.97 ppm, which will be discussed below.

As the extent of suppression depends on the difference in Larmor frequency of the two coupled nuclei, the method is very efficient when a short  $\tau_{\text{SL}}$  (e.g. 5–10 ms) is used for the suppression of ZQC in the fingerprint region, but it becomes less effective as the diagonal is approached. An example of this is shown in Fig. 3, where the effectivity of the suppression of ZQC between  $\beta$ -protons in the aliphatic region is compared. In principle, the ZQC are only partially dephased in a region around the diagonal, whose width is determined by the duration of the spin lock according to Eqs. 7 and 8.

The measurement of distances by means of quantitative evaluation of NOESY spectra is usually based on a set of spectra recorded with short mixing times (Kumar et al., 1981). As shown in Eq. 10, the similarity of the build-up rates of an uncompensated and a compensated experiment

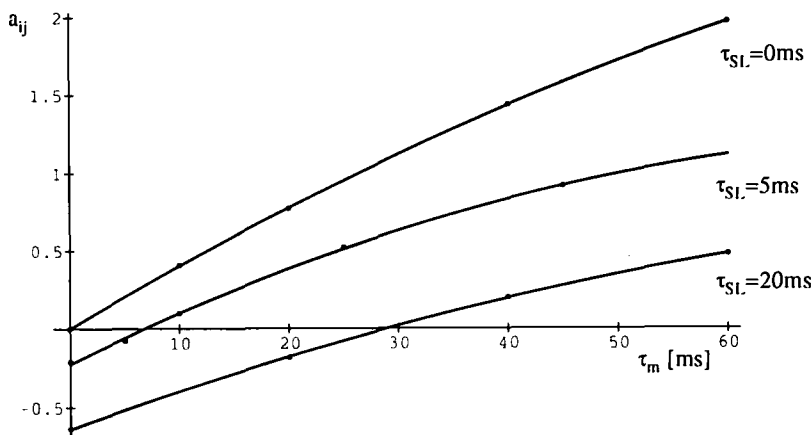


Fig. 4. Build-up curves for the cross peak involving the  $C_{\alpha}H$  of Val<sup>34</sup> and the NH of Tyr<sup>35</sup> measured by uncompensated NOESY ( $\tau_{SL} = 0$  ms) and ZQC-compensated NOESY ( $\tau_{SL} = 5, 20$  ms) fitted to a quadratic term. The amplitudes are given in arbitrary units, the error on the individual points was estimated to be  $\pm 0.02$ . The distances obtained in the ZQC-compensated NOESY experiments differed by less than  $0.05 \text{ \AA}$  from those obtained in an uncompensated NOESY (see also Table 1).

depends on the duration of the spin lock. As an example, the build-up curve for the cross peak between the NH of Tyr<sup>35</sup> and the  $C_{\alpha}H$  of Val<sup>34</sup>, recorded with a normal NOESY sequence, is compared in Fig. 4 with that of compensated experiments at spin-lock times of 5 ms and 20 ms. The curves shown were obtained by fitting the data to a second-order polynomial expression. The linear slope with respect to  $\tau_m$  shows a systematic, but small, decrease for increasing  $\tau_{SL}$ , as predicted from Eq. 11 (see also Table 1). In addition, a different deviation of the build-up curves from linearity is observed. This is due to interference of second-order terms in  $\tau_m$  and  $\tau_{SL}$ , which is not accounted for in our analysis. This was observed over the whole spectrum. However, accurate distances can be deduced from the linear slope, as shown in Table 1, for some typical cross peaks. Although the linear terms of the quadratic fit varied in a systematic manner, the effects on the distances were smaller than  $0.05 \text{ \AA}$ .

For proteins, the build-up starts with a negative intensity. This may mean that a positive amplitude is not reached for some cross peaks, even with a long  $\tau_m$ . Examples are the cross peaks of Thr<sup>11</sup> at 4.01/8.97 ppm and 4.89/8.97 ppm, and the cross peak of Arg<sup>39</sup> at 3.90/9.08 ppm, which were absent in the compensated experiment of Fig. 2B at a NOE mixing time of  $\tau_m = 30$  ms. In spectra with short  $\tau_m$ , negative cross peaks are present. The reason is the very efficient transverse relaxation during the spin-lock time in the compensated experiment. It causes an earlier deviation of the build-up curve from linearity than in an uncompensated experiment. However, our sample shows extraordinarily broad NH resonances for the Arg<sup>39</sup> and Thr<sup>11</sup> residues. Their build-up curves reflect attenuation by transverse relaxation and explain the zero amplitude at longer mixing times  $\tau_m$ .

The discussion and theory so far are only valid for the pulse sequences of Figs. 1A–1C. In principle, it should be possible to introduce two spin-lock times, one before and one after the NOESY mixing time. This experiment is shown in Fig. 1D and results in the suppression of ZQC with the same efficiency as the compensated sequences in Figs. 1A–1C for  $\tau_{SL}^1 + \tau_{SL}^2 = \tau_{SL}$ , since ZQC arise in the NOESY experiment only from antiphase magnetization during the evolution

period,  $t_1$ . However, the separation of the spin-lock period into two phases causes a further transfer of magnetization during the mixing process and results in a more complicated distribution of the magnetization of spin  $i$  across the spin system, making a quantitative evaluation of the build-up more difficult.

With the proposed method, a single experiment establishes ZQC suppression, but the distance determination requires a build-up curve and therefore 2–4 experiments. In comparison, ZQC suppression by varying the effective precession period of ZQC during a fixed NOESY mixing time (Rance et al., 1985; Otting 1990) requires several experiments (at least 2), but it may be possible to determine the distances from only one NOESY spectrum with a short  $\tau_m$ . Both methods may therefore require a similar total measurement time. However, during spin locking, all coherences, except the locked in-phase magnetization, are dephased due to RF inhomogeneity (see Introduction). The proposed ZQC-compensated experiment may therefore be performed with a two-step phase cycle for the suppression of axial peaks. The ZQC are only suppressed inside a frequency band  $\Delta\Omega_{ZQ \min} < \Delta\Omega_{ZQ} < \Delta\Omega_{ZQ \max}$  of given bandwidth  $|\Delta\Omega_{ZQ \max} - \Delta\Omega_{ZQ \min}|$ , when experiments with different effective precession periods for ZQC are added. The number of experiments necessary to achieve sufficient ZQC suppression increases with the bandwidth. The ZQC in the

TABLE I  
THE EFFECT OF THE SPIN-LOCK PERIOD IN THE ZQC-COMPENSATED NOESY EXPERIMENT WITH BPTI ON THE DETERMINATION OF INTERNUCLEAR DISTANCES OF CROSS PEAKS IN THE FINGER-PRINT REGION<sup>a</sup>

NOE	34HA/35HN	32HA/33HN	49HA/49HN	30HA/31HN
Distance <sup>b</sup> (Å) taken from X-ray	2.082	2.189	2.878	2.148
Slope when $\tau_{SL} = 0$ ms	418	273	104	304
Distance (Å)	2.035	2.235	2.638	2.198
Slope when $\tau_{SL} = 5$ ms	345	206	086	263
Distance (Å)	2.117	2.269	2.624	2.178
Slope when $\tau_{SL} = 20$ ms	253	149	075	197
Distance (Å)	2.110	2.274	2.550	2.171

<sup>a</sup> The distances obtained from one series of uncompensated NOESY experiments ( $\tau_{SL} = 0$  ms) and two series of ZQC-compensated NOESY experiments ( $\tau_{SL} = 5$  ms and  $\tau_{SL} = 20$  ms) are compared. The respective mixing times ( $\tau_m$ ) are listed in the experimental section. The build-up curves for the 34HA/35HN cross peak are shown in Fig. 4. The integrated intensities of the cross peaks as a function of the mixing time  $\tau_m$  were fitted to a quadratic term. The distances were calculated from the linear term, assuming that the linear slope of the build-up curve of a cross peak between the nuclei  $i$  and  $j$  is proportional only to  $(r_{ij})^{-6}$  (for the ZQC-compensated NOESY experiments this holds rigorously in the limit  $\tau_{SL} \rightarrow 0$  ms). The slope of the build-up curve for the 34HA/35HN cross peak in the series of uncompensated NOESY experiments was taken as a reference (2.082 Å)<sup>b</sup> for the determination of all other distances. However, the distance between the 34HA and 35HN was obtained by using the slope for the 30HA/31HN cross peak from the series of uncompensated NOESY experiments as reference (2.148 Å)<sup>b</sup>.

<sup>b</sup> The distances were determined from the X-ray structure 4PTI (Marquart et al., 1983) of the Brookhaven data bank after adding protons to the carbon skeleton followed by a short energy minimization (Brünger 1992), in which the coordinates of the carbon skeleton were not changed.

fingerprint region, for example, are reduced to 15% of their maximal intensity by 4 extra experiments (Rance et al., 1985). Outside this region, the ZQC are much less attenuated or are even not attenuated. In the proposed ZQC-compensated experiment, the signals are suppressed in the whole spectrum, except for a region of width  $6/\tau_{\text{SL}}$  around the diagonal.

## CONCLUSION

Efficient ZQC suppression in NOESY spectra of proteins can be achieved in one scan by using the natural cw RF inhomogeneity of commercial probes. As the extent of suppression depends on the difference between the Larmor frequency of the two coupled nuclei, the method is very efficient when short  $\tau_{\text{SL}}$  (e.g., 5–10 ms) are used to suppress ZQC in the fingerprint region of protein spectra, but becomes less efficient in the region around the diagonal. The application of this method to small proteins for the measurement of distances is straightforward, provided a  $\tau_{\text{m}}$  series starting at zero mixing time is recorded and a moderate length is chosen for the spin lock. For larger proteins, where the transverse relaxation time is close to the spin-lock times used here (5–10 ms), the compensated NOESY experiment yields build-up curves with very short or even no linear dependence on  $\tau_{\text{m}}$ . (In this case, and for ZQC suppression very close to the diagonal, a modified probe with an enhanced RF inhomogeneity may be used.)

## ACKNOWLEDGEMENTS

We thank G. Estcourt for helpful discussions.

## REFERENCES

- Abraham, A. (1961) *Principles of Nuclear Magnetism*, Oxford University Press, Oxford, pp. 34–36.
- Bax, A., De Jong, P.D., Mehlkopf, A.F. and Smidt, J. (1980) *Chem. Phys. Letters*, **69**, 567–570.
- Bax, A. (1982) *Two-Dimensional Nuclear Magnetic Resonance in Liquids*, Delft University Press, Delft, p. 25.
- Bazzo, R. and Boyd, J. (1987) *J. Magn. Reson.*, **75**, 452–466.
- Bodenhausen, G. (1981) *Progr. NMR Spectr.*, **14**, 137–173.
- Bodenhausen, G., Kogler, H. and Ernst, R.R. (1984) *J. Magn. Reson.*, **58**, 370–388.
- Brünger, A. (1992) X-PLOR (VERSION 3.0) Manual, New Haven.
- Griesinger, C. and Ernst, R.R. (1987) *J. Magn. Reson.*, **75**, 261–271.
- Hardy, C.J., Edelstein, W.A. and Vatis, D. (1986) *J. Magn. Reson.*, **66**, 470–482.
- Kumar, A., Wagner, G., Ernst, R.R. and Wüthrich, K. (1981) *J. Am. Chem. Soc.*, **103**, 3654–3658.
- Macura, S., Huang, Y., Suter, D. and Ernst, R.R. (1981) *J. Magn. Reson.*, **43**, 259–281.
- Marquart, M., Walter, J., Deisenhofer, J., Bode, W. and Huber, R. (1983) *Acta Crystallogr. Sect. B*, **39**, 480–490.
- Otting, G. (1990) *J. Magn. Reson.*, **86**, 496–508.
- Rance, M., Bodenhausen, G., Wagner, G., Wüthrich, K. and Ernst, R.R. (1985) *J. Magn. Reson.*, **62**, 497–510.
- Sørensen, O.W., Rance, M. and Ernst, R.R. (1984) *J. Magn. Reson.*, **56**, 527–534.
- Titman, J.J., Davis, A.L., Laue, E.D. and Keeler, J. (1990) *J. Magn. Reson.*, **89**, 176–183.
- Ugurbil, K., Garwood, M. and Rath, A.R. (1988) *J. Magn. Reson.*, **80**, 448–469.
- Wokaun, A. and Ernst, R.R. (1977) *Chem. Phys. Letters*, **52**, 407–412.